

# O(g) Plasma Effects in Jet Quenching

Simon Caron-Huot<sup>†</sup>

<sup>†</sup> Department of physics, McGill University, Montréal, Canada.  
scaronhuot@physics.mcgill.ca

## Abstract

We consider the bremsstrahlung energy loss of high energy partons moving in the quark-gluon plasma, at weak coupling. We show that the rates for these processes receive large O(g) corrections from classical (nonabelian) plasma physics effects, which are calculated. In the high-energy (deep LPM) regime these corrections can be absorbed in a change of the transverse momentum broadening coefficient  $\hat{q}$ , which we give to the next-to-leading order. The correction is large even at relatively weak couplings  $\alpha_s \sim 0.1$ , as is typically found for such effects, signaling difficulties with the perturbative expansion. Our approach is based on an effective “Euclideanization” property of classical physics near the light-cone, which allows an effective theory approach based on dimensional reduction and suggests new possibilities for the nonperturbative lattice study of these effects.

# 1 Introduction

The phenomenon of jet quenching, or suppression of high- $p_T$  hadrons in  $A+A$  collisions relative to expectations from scaling of binary  $p+p$  collisions, has been the focus of much recent interest in RHIC physics [1] [2]. Its theoretical description ([3] and references therein) is based on the theory of jet evolution in thermalized media, whose uncertainties it is thus worthwhile to seek to reduce, or at least, quantify. This requires the calculation of higher-order effects, which we propose to do in this paper in the regime of weak coupling.

As established by a large body of work on the thermodynamic pressure [4] [5] [6], finite temperature perturbation theory meets with serious convergence difficulties. Unless the strong coupling  $\alpha_s$  obeys  $\alpha_s \lesssim 0.1$ , strict perturbation theory in powers of  $g$  is unreliable. Such a behavior seems generic: it is also observed for the next-to-leading order (NLO,  $\mathcal{O}(g)$ ) corrections to thermal masses [7] [8] [9], as well as for the only transport coefficient presently known at NLO, heavy quark momentum diffusion [10] (whose behavior appears even worse).

Following Braaten and Nieto [5], who studied the thermodynamic pressure, these large perturbative corrections can be attributed to purely classical (nonabelian) plasma effects. They have shown this by first making use of the scale separation  $gT \ll 2\pi T$  to integrate out the scale  $2\pi T$ , leaving out a three-dimensional effective theory (“electric QCD”, or EQCD) describing the scale  $m_D \sim gT$  as well as more infrared scales. The claim is then that contributions from the scale  $2\pi T$ , as well as the parameters of the effective theory, enjoy well-behaved perturbative series [5] [11]; all large corrections are included in the effective theory. Furthermore, by treating this effective theory nonperturbatively using various resummation schemes [9] [12] or the lattice [13], reasonable convergence can be obtained down to  $T \sim 3 - 5T_c$ .

It is natural to expect large corrections from  $gT$ -scale plasma effects in other quantities as well. Unfortunately, for real time quantities such as most transport coefficients and collision rates, a resummation program similar to that available in Euclidean space has yet to be fully developed and applied. This is because the real-time description of plasmas requires the hard thermal loop (HTL) theory [14] (which in essence is classical (nonabelian) plasma physics [15], also known as the Wong-Yang-Mills system [16]), which is arguably more complicated than its Euclidean counterpart EQCD.

In this paper, we aim to point out progress which can be made for a specific class of “real-time” quantities: those which probe physics near the light cone. This includes the collision kernel  $C(q_\perp)$  that is relevant for the transverse evolution of jets, whose crucial role in the theory of jet quenching will be reviewed below.

To explain the idea, we first observe that the soft contribution to  $C(q_\perp)$  (that arising from soft collisions with  $q_\perp \sim gT$ ) is described by soft classical fields that are being probed passively by the high-energy jet passing through them. These soft

classical fields are the fields surrounding the plasma particles. At this point we observe that field components moving collinearly with the jet are not particularly important — the standard calculation of collision rates [17] (or see eq. (22) below) reveals that the contributing particles move with generic angles in the plasma frame, with even a suppression for the ones collinear to the jet (due to the reduced center-of-mass energy) — which implies that the result must be insensitive to the precise value of the jet velocity  $v \approx 1$ . The trick is then to think of  $v$  as  $v = 1 + \epsilon$  — which, though unphysical, doesn't affect the answer — thus making the hard particle's trajectory *space-like*. This makes Euclidean techniques directly applicable including dimensional reduction, as will be explained below, thereby dramatically simplifying the calculation.

In this paper we will thus (analytically) compute the full  $\mathcal{O}(g)$  corrections to the transverse collision kernel  $C(q_\perp)$ , describing the evolution of the transverse momentum of a fast particle. The second moment of that kernel gives the phenomenologically interesting momentum broadening coefficient  $\hat{q}$ , which we also compute at NLO.

This paper is organized as follows. In section 2 we summarize our results and explain their relevance to jet quenching; in particular we discuss the relevance of the parameter  $\hat{q}$ . In section 3 we explain our computational strategy and formalism. Details of the calculation of  $C(q_\perp)$  and of its (ultraviolet-regulated) second moment  $\hat{q}$  are given in sections 4 and 5, respectively. In section 6 we derive, at NLO, the relation between the collision kernel  $C(q_\perp)$  for momentum broadening and that for jet evolution — which turns out to be identical to the leading-order relation — and we discuss certain operator ordering issues which could enter higher-order treatments. Finally, in Appendix A we relate our approach to a slight generalization of sum rules previously found by Aurenche, Gelis and Zaraket [18].

Alternative estimates of  $\hat{q}$  and of jet evolution, based on gauge-string duality (see for instance [19, 20] [21] [22] [23] [24] [25]), will not be discussed in this paper.

## 2 Results

### 2.1 Collision kernel

The main result of this paper is the full next-to-leading order ( $\mathcal{O}(g)$ ) (analytic) expression (20) for the two-body collision kernel  $C(q_\perp)$ , defined as:

$$\frac{d\Gamma}{d^2q_\perp/(2\pi)^2} \equiv C(q_\perp), \quad (1)$$

describing the evolution of the transverse momentum of a hard particle (with  $E \gtrsim T$ ).

The  $\mathcal{O}(g)$  corrections to  $C(q_\perp)$ , which being due to  $gT$ -scale physics only arise for  $q_\perp \sim gT \ll T$ , are illustrated in fig. 1. Both the LO and NLO kernels  $C(q_\perp)$  are proportional to the (quadratic) Casimir of the gauge group representation of the jet.

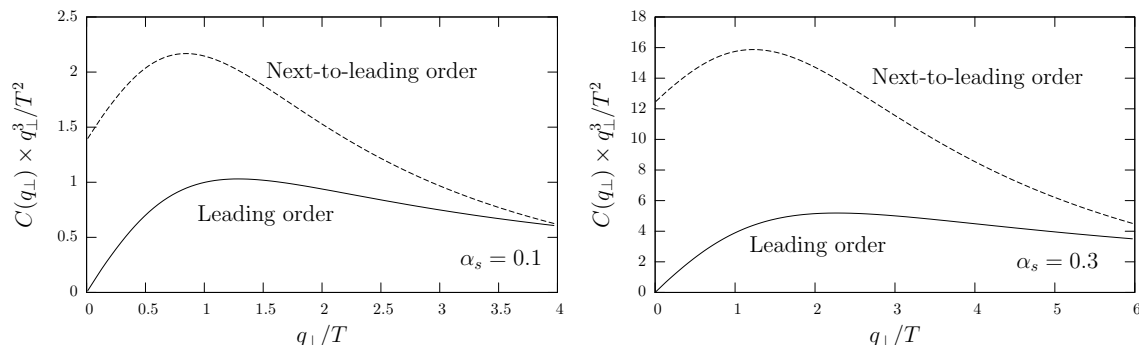


Figure 1: LO and NLO collision kernels  $C(q_\perp) \equiv (2\pi)^2 d\Gamma/d^2q_\perp$  for a fast quark in QCD (with  $N_f = 3$ ), for  $\alpha_s = 0.1$  and  $\alpha_s = 0.3$ . For gluons the curves are to be multiplied by a (Casimir) factor  $9/4$ .

The “leading order curves” is based on the full (unscreened) expression (22) at hard momenta, multiplied by  $q_\perp^2/(q_\perp^2 + m_D^2)$  to make it merge smoothly with the analytic result (10) at low momenta, following the prescription given in [26]. The “next-to-leading order” curves use the leading order curves plus  $C(q_\perp)^{(\text{NLO})}$  given in (20).

The NLO correction is already quite large for  $\alpha_s = 0.1$ , giving nearly a factor of 2 around  $q_\perp \approx T$ . As discussed in the Introduction, this is consistent with the behavior observed for  $\mathcal{O}(g)$  effects in other quantities. At  $\alpha_s = 0.3$ , a typical value used in comparisons with RHIC data (see e.g. [27]), it is clear that the strength of the correction has grown out of control, meaning that (presently unknown) yet higher-order corrections are most certainly also important (though our results suggest that the value of  $\alpha_s$  needed to fit the data might be significantly smaller than the estimate of [27]).

An interesting by-product of the approach used in this paper is that it extends naturally to higher orders: it makes perfect sense to evaluate the gauge-invariant Wilson loop (9) nonperturbatively within the *Euclidean* three-dimensional EQCD theory, for instance using the lattice. Although this may not include *all*  $\mathcal{O}(g^2)$  corrections to  $C(q_\perp)$  (contributions from the hard scale  $2\pi T$  will be missed), by analogy with the works on the pressure discussed in the Introduction, these missing contributions can be expected to be numerically suppressed<sup>1</sup>. We leave to future work the study of this interesting possibility.

<sup>1</sup>Their description could turn out to be very complicated, though, because jet evolution at  $\mathcal{O}(g^2)$  should contain, among other things, the analog of the NLO vacuum DGLAP splitting amplitudes in the presence of the LPM effect (described below). Also, various effects involving the scale evolution of the medium constituents and coupling constant evolution should arise.

## 2.2 Application to Jet Evolution

The dominant energy loss mechanism of high energy particles (at weak coupling) is bremsstrahlung (including quark-antiquark pair production), triggered by soft collisions against plasma constituents. The theoretical description of these processes, at the leading order in the coupling, is well-established [28] [29] [30]. Their duration  $t_{\text{form}}$  depends on the energy of the participants, and can interpolate between the Bethe-Heitler (single scattering) regime  $t_{\text{form}} \sim E/q_{\perp}^2 \sim E/m_D^2$  at energies  $E \lesssim T$ , and the Landau-Pomeranchuk-Migdal (LPM) [31] (multiple-scattering) regime at high energies  $E \gg T$ , with  $t_{\text{form}} \sim \sqrt{E/\hat{q}}$ , in which destructive interference between different collisions plays a significant role.

In all of these regimes, however, the description factors into a “hard” collinear splitting vertex (Dokshitzer-Gribov-Lipatov-Altarelli-Parisi, DGLAP vertex [33]), times an amplitude (wavefunction in the transverse plane) which describes the in-medium evolution of the vertex. The latter accounts for the collisions which trigger, and occur during, the splitting process [28] [29] [30]. The DGLAP vertices themselves only involves hard scale physics (in essence, they are Clebsch-Gordon coefficients between states of different helicities) and thus cannot receive  $\mathcal{O}(g)$  corrections; the NLO effects, which come from soft classical fields with  $p \sim gT$ , are included in their dressing amplitude.

In section 6 we discuss these amplitudes at NLO and show that the relevant (three-body) collision kernel factors as a sum of two-body kernels  $C(q_{\perp})$ , exactly like the LO one does [28] [29] [30, 32]. As a consequence, our results can be used to give a full NLO treatment of radiative jet energy loss; one must simply include the NLO shift (20) to the two-body kernel  $C(q_{\perp})$  which serves as an input to these calculations<sup>2</sup>.

## 2.3 Momentum broadening coefficient ( $\hat{q}$ )

When the effects of a large number of small collisions are added together, it is natural to replace them by an effective diffusive process. The diffusion coefficient relevant for transverse momentum broadening,  $\hat{q}$ , is defined as the second moment of the collision kernel (1):

$$\hat{q} \equiv \int_0^{q_{\text{max}}} \frac{d^2 q_{\perp}}{(2\pi)^2} q_{\perp}^2 C(q_{\perp}). \quad (2)$$

The ultraviolet cutoff  $|q_{\perp}| < q_{\text{max}}$  is needed to deal with the weak power-law falloff  $C(q_{\perp}) \sim g^4 T^3 / q_{\perp}^4$  at large  $q_{\perp}$ , which leads to a logarithmic dependence of  $\hat{q}$  on  $q_{\text{max}}$ . This is a *leading order* logarithm; below we shall comment on the value of the cutoff  $q_{\text{max}}$ . Using our NLO kernel (20) we can calculate the expansion of  $\hat{q}$  up to terms of

---

<sup>2</sup> For instance, one would simply modify “ $C(q_{\perp})$ ” in [32], which is actually equal to  $C(q_{\perp})/(g^2 C_s T)$  in our conventions.

order  $g^2$  <sup>3</sup>:

$$\begin{aligned} \frac{\hat{q}}{g^4 C_s T^3} &= \frac{C_A}{6\pi} \left[ \log \left( \frac{T}{m_D} \right) + \frac{\zeta(3)}{\zeta(2)} \log \left( \frac{q_{\max}}{T} \right) - 0.068854926766592 \dots \right] \\ &+ \frac{N_f T_f}{6\pi} \left[ \log \left( \frac{T}{m_D} \right) + \frac{3}{2} \frac{\zeta(3)}{\zeta(2)} \log \left( \frac{q_{\max}}{T} \right) - 0.072856349715786 \dots \right] \\ &+ \frac{C_A m_D}{6\pi T} \xi^{(\text{NLO})} + \mathcal{O}(g^2), \end{aligned} \quad (3)$$

with  $\xi^{(\text{NLO})} = \frac{3}{16\pi} (3\pi^2 + 10 - 4 \log 2) \simeq 2.1985$  a constant calculated in section 5, characterizing the NLO correction to  $\hat{q}$ , and  $m_D^2 = g^2 T^2 (N_c + N_f T_f)/3$  the leading-order Debye mass. In QCD with  $N_f = 3$  flavors of fundamental quarks,  $C_A = 3$  and  $N_f T_f = 1.5$ . For a discussion of the leading order result and logarithms, we refer the reader to P. Arnold's work [26], from which the high-precision numbers were taken.

The series (3) is meant to represent the expansion in  $g$  of the area under the curve of plots such as fig. 1. For  $\alpha_s = 0.1$  and a quark ( $C_s = \frac{4}{3}$ ) the area under the leading order curve in the figure (up to  $q_{\max} = 4T$ ) would yield  $\hat{q}^{\text{LO}} \approx 2.60 \text{ (T/GeV)}^3 \text{ GeV}^2/\text{fm}$  whereas the first two lines of (3) give  $\hat{q}^{\text{LO,th}} \approx 2.08 \text{ (T/GeV)}^3 \text{ GeV}^2/\text{fm}$ . The NLO shift is  $\Delta\hat{q} \approx 2.22 \text{ (T/GeV)}^3 \text{ GeV}^2/\text{fm}$  from the figure, about a factor of two effect, and  $\Delta\hat{q}^{\text{th}} \approx 5.26 \text{ (T/GeV)}^3 \text{ GeV}^2/\text{fm}$  according to (3). Thus the third line of (3) itself suffers from sizeable truncation errors compared to our full NLO result (20). We would like to stress, however, that (20), and fig. 1, is not merely a simple truncation error from a lower-order contribution but represents a genuine NLO effects.

As discussed in the preceding subsection, it would be premature to attempt comparison of our  $\hat{q}$  results with experimental data, since it is clear that (yet unknown) higher-order corrections should also be important at physically relevant couplings. It is also worth noting that different approximation schemes taking  $\hat{q}$  as input (this excludes the AMY scheme [30, 32], which uses the full  $C(q_\perp)$ ) when fitted to RHIC data, tend to disagree rather significantly on its preferred value [3]; since a critical analysis of these approximations lies beyond our scope, this simply means it is not completely clear which experimentally-extracted value of  $\hat{q}$  we should comparing with.

It seems appropriate here to recall some subtleties associated with the phenomenological parameter  $\hat{q}$ , which do not arise if one instead works with the full collision kernel  $C(q_\perp)$ . First, the value of the cutoff  $q_{\max}$  to be used in (3) is process-dependent: since the  $q_\perp > q_{\max}$  tail of  $C(q_\perp)$  describes collisions occurring on a finite rate<sup>4</sup>  $\Gamma_{(q_\perp > q_{\max})} \sim g^4 T^3 / q_{\max}^2$ , weighting them with  $q_\perp^2$  in (23) ceases to make sense for  $\Gamma_{(q_\perp > q_{\max})}^{-1} \gtrsim t_{\text{jet}}$ , with  $t_{\text{jet}}$  the jet's lifetime, to be replaced with a formation time  $t_{\text{form}}$  for bremsstrahlung pairs in the context of energy loss calculations. Therefore, parametrically, one should

<sup>3</sup>Version 1 of the present paper contained a transcription error which is now corrected in (3). The argument of the logarithm (incorrectly) read  $q^*$  as opposed to  $m_D$  obtained from (23) and (24).

<sup>4</sup>I am indebted to G. D. Moore for this discussion.

set  $q_{\max} \sim \sqrt{g^4 T^3 t_{\text{jet}}}$ . For bremsstrahlung in the deep LPM regime,  $t_{\text{jet}} \rightarrow t_{\text{form}} \sim \sqrt{E/\hat{q}}$  so  $q_{\max} \sim g(ET^3)^{1/4}$  [34]<sup>5</sup>.

Second, the presence of the ultraviolet tail implies that collisions having  $q_{\perp} \sim q_{\max}$  (with  $q_{\max}$  the physical cutoff as determined above), which are intrinsically non-diffusive, already contribute at the next-to-leading logarithm order to bremsstrahlung rates. That is, they contribute at  $\mathcal{O}(1)$  compared to the log-enhanced diffusive contribution  $\sim \log q_{\max}/m_D$  coming from  $m_D \ll q_{\perp} \ll q_{\max}$ . Therefore, approximations based on diffusive physics lead, at best, to expansions in inverse logarithms of the energy. Such expansions were systematically studied in [34], with the conclusion that formulae to *next-to-leading* logarithm can be trusted at least when  $E_{\text{jet}} \gtrsim 10T$ , with the inclusion of the subleading term (e.g. the constant under the logarithm) being mandatory. None of the presently applied approaches which rely on  $\hat{q}$  as a phenomenological parameter presently includes such subleading logarithms (see [3, 35] and references therein for an overview of these approaches).

### 3 Strategy: Space-like Correlators and EQCD

In this section, we relate certain correlators at space-time separation (more precisely, correlators supported on space-like, and light-like, hyperplanes of the type  $x^0 = \tilde{v}x^3$ ,  $\tilde{v} \leq 1$ ), to Euclidean-signature correlators. We will then apply to them the formalism of dimensional reduction.

#### 3.1 Space-like correlators

Field operators at space-like separated points (anti)commute with each other and their correlator does not depend on the operator ordering. For two-point functions at vanishing time separation, a well-known Euclidean representation holds [36]:

$$G_{ij}^>(t=0, \mathbf{x}) \equiv \frac{1}{\text{Tr } e^{-\beta H}} \text{Tr } e^{-\beta H} \mathcal{O}_i(\mathbf{x}) \mathcal{O}_j(0) = T \sum_n \int \frac{d^3 \mathbf{p}}{(2\pi)^3} e^{i\mathbf{p} \cdot \mathbf{x}} G_E(\omega_n, \mathbf{p}), \quad (4)$$

with the sum running over the Matsubara frequencies  $\omega_n = 2\pi i n T$ ,  $\beta = 1/T$ , and with  $G_{ij}^E$  the Euclidean correlator of some operators  $\mathcal{O}_{i,j}$  taken here to be bosonic.

In Lorentz-covariant theories, (4) can be extended immediately to any correlator which is equal-time in a suitable boosted frame. Specifically, under a  $z$ -axis boost with velocity  $\tilde{v}$ , the thermal density matrix transforms to:

$$e^{-\beta H} \rightarrow e^{-\tilde{\gamma}\beta(H' + \tilde{v}P'^3)}, \quad (5)$$

---

<sup>5</sup> This should be contrasted with the often-used kinematic cutoff  $q_{\max}^2 \approx ET$ .

the primed quantities referring to quantities in the boosted frame;  $\tilde{\gamma} = \frac{1}{\sqrt{1-\tilde{v}^2}}$ . The identification of  $H'$  and  $P'^3$  as the generators of time and space translation shows periodic identification  $x'^\mu = x'^\mu + i\tilde{\gamma}(\beta, -\tilde{v}\beta, 0_\perp)$  for the geometry associated to (5), with associated quantization condition on the “Matsubara frequencies”  $p'^0 + \tilde{v}p'^3 = 2\pi i n T / \tilde{\gamma}$ . The spatial momentum  $p'^3$  must be kept real: it serves as a label for the physical states living on the  $x'^0 = 0$  hyperplane. Thus only the frequency  $p'^0$  is complex. This determines the extension of (4) to equal-time two-point functions in the boosted frame:

$$G_{ij}^>(x'^0 = 0, \mathbf{x}') = \frac{T}{\tilde{\gamma}} \sum_n \int \frac{d^3 \mathbf{p}'}{(2\pi)^3} e^{i\mathbf{p}' \cdot \mathbf{x}'} G_E(p_n'^0, \mathbf{p}'), \quad p_n'^0 = -\tilde{v}p'^3 + 2\pi i n \frac{T}{\tilde{\gamma}}. \quad (6)$$

It will be convenient to boost this formula back to the plasma rest frame, and to write it for general space-time arguments ( $\tilde{v} = \frac{x^0}{x^3}$ ):

$$G_{ij}^>(x^0, \mathbf{x}') = T \sum_n \int \frac{d^3 \mathbf{p}}{(2\pi)^3} e^{-i(p_n^0 x^0 - p_n^3 x^3 - p_\perp \cdot x_\perp)} G_{ij}^E(p_n^0, p_n^3, p_\perp),$$

$$p_n^0 = 2\pi i n T, \quad p_n^3 = p^3 + 2\pi i n T \frac{x^0}{x^3}. \quad (7)$$

Eq. (7) is the main result of this section. It differs from (4) only due to the imaginary part of  $p_n^3$ , which, in fact, is required for the convergence of the sum over  $n$ : it prevents the Fourier exponential to contain exponentially growing terms as opposed to pure phases. Eq. (7) extends in a straightforward way to any higher-point correlator supported on  $(\frac{x^0}{x^3} = \tilde{v})$ -type hyperplanes: one gets a summation-integration  $\sum_n \int_p$ , with the  $p_n$  as in (7), for all external legs, subject to the usual restriction of momentum conservation (and thus of “ $n$  conservation”), as for equal-time higher-point correlators [36]. The momenta running in loops must also be “twisted” like those in (7), e.g.  $\text{Im } p^3 = \tilde{v} \text{Im } p^0$ , to reflect the boosted-frame origin of the formula<sup>6</sup>. This ensures that the imaginary part of every momentum is time-like, which is the natural domain of Euclidean physics.

We will be interested in the amplitudes of ultrarelativistic dipoles moving with velocity  $v = 1$ , e.g.  $x^3 = x^0$  (note  $\tilde{v} = 1/v$  in general). Our derivation of (7) might seem compromised, since an “infinite” boost with velocity  $\tilde{v} = 1$  obviously doesn’t exist. However, a more careful look at the argument reveals that the boost plays no important role: after all we un-did it in the end. All that is really important, is that we can imagine quantizing the system along hyperplanes parallel to  $\tilde{v}$ , and express the thermal density matrix within these hyperplanes. Since it is certainly possible to quantize a system along light fronts, the result (7) must hold for  $x^3 = x^0$ . An alternative derivation of this, based on sum rules, is also given in App. A.

---

<sup>6</sup> Note that this gives an implicit dependence on the velocity  $v$  to  $G_{ij}^E(p_n^0, p_n^3, p_\perp)$  appearing in (7).



The attentive reader might complain that setting  $x^3 = x^0$  in (7) corresponds to taking a  $v \searrow 1$  limit, whereas the physically relevant regime  $v \nearrow 1$  lies beyond the reach of (7). Are we claiming that these limits are equivalent in general? No<sup>7</sup>. Our claim, explained in the introduction, is merely that for *classical* plasma physics effects they are equivalent — to the extent that the observable of interest is only passively probing a soft classical background, only a phase-space suppressed fraction of which propagates collinearly with the jet, this seems to be rather robust. It is unclear whether this will remain true when quantum effects are included (which will enter at  $\sim g^2$ ), though, because of collinear components present in the jet’s own wavefunction.

### 3.2 Dimensional reduction

Naturally, the contribution from soft physics (momenta  $\sim gT$ ) to sums like (7) is expected to be dominated by the  $n = 0$  mode. We will thus begin by “integrating out” the modes with  $n \neq 0$ .

First we claim that loop diagrams for which all external momenta have  $n = 0$  are equal to the standard ones. These two sets of diagrams have  $p^0 = 0$  and  $p_z$  real, and could only differ due to the “twisted” Matsubara momenta (7) which circulate in the former; our claim is that this does not affect their value. The reason is that the imaginary part of every momentum  $P$  in such loops is time-like with a real part obeying  $\text{Re } p^0 = 0$ , ensuring that  $\text{Re } P^2$  is positive-definite. The imaginary part of the  $p^3$  integration contours can thus be deformed from  $\text{Im } p^3 = \tilde{v} \text{Im } p^0$  to  $\text{Im } p^3 = 0$ , without crossing any pole.

In particular, the modes with  $n = 0$  are described by precisely the standard “electric QCD” (EQCD) three-dimensional effective theory [37, 38]. EQCD is pure three-dimensional Yang-Mills with coupling constant  $g_3^2 = g^2 T$  coupled to a massive adjoint scalar  $A_0$  of mass  $m_D$ . It is an effective theory for the  $gT$  scale (the Euclidean version of the hard thermal loop theory [14]), in which the loop expansion proceeds in powers of  $g^2 T / m_D \sim g$ . Its parameters do not receive  $\mathcal{O}(g)$  corrections.

---

<sup>7</sup> In strongly coupled theories accessible to gauge-string duality, these two limits are known to be physically distinct. A calculation of  $\hat{q}$  for a physical massive quark moving with  $v < 1$  (in the sense of its momentum broadening coefficient) by Teaney and Casalderrey-Solana [21], and by Gubser [22], found a divergence  $\hat{q} \sim (1 - v^2)^{-1/4} \sqrt{\lambda} T^3$  as  $v \nearrow 1$ . This calculation is valid for energies  $E < M^3 / \lambda T^2$ , beyond which the coherence time of the force acting on the quark becomes of order the time scale of Langevin dynamics [22]; a time-independent description is then impossible. This suggests that  $\hat{q}$  for  $v < 1$  should depend on a cutoff time scale, as is the case at weak coupling.

On the other hand, the  $v \searrow 1$  limit has been studied by Rajagopal, Liu and Wiedemann [19, 20], by embedding Euclidean worldsheets into  $\text{AdS}_5$  space, and no divergences were met in this limit. It is thus qualitatively quite distinct.

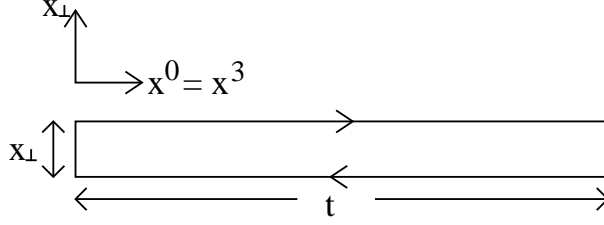


Figure 2: Wilson loop representation of the dipole amplitude.

The propagators of EQCD are:

$$\tilde{G}^{00}(q) = \frac{-1}{q^2 + m_D^2}, \quad \tilde{G}^{ij}(q) = \frac{\delta^{ij}}{q^2} - \frac{\xi q^i q^j}{q^4}. \quad (8)$$

(We use the tilde to denote that these are three-dimensional propagators.) The minus sign in front of the  $A^0$  propagator reflects the fact that we will couple it to Minkowski-space Wilson lines: we have *not* performed a Wick rotation.

In addition to its interaction with the  $n = 0$  modes, we must also include the direct coupling of the operator of interest to the  $n \neq 0$  modes. Physically, and as shown in Appendix A, a contribution from these modes would correspond, in the real-time formalism, to a failure of the soft approximation  $n_B(p^0) \approx T/p^0$ . Such a failure would signal a contribution from the  $p^0 \sim T$  region in Minkowski space, which would necessary be signaled by ultraviolet divergences in the soft approximation, since this approximation correctly describes the intermediate region  $gT \ll p^0 \ll T$  and any contribution from the scale  $T$  should leave an imprint on this region. Thus, provided we do not find ultraviolet divergences from the  $n = 0$  contribution alone (which computes exactly the soft approximation, see Appendix A), this argument shows that we can safely ignore the direct coupling to the  $n \neq 0$  modes. This will turn out to be our case.

## 4 The calculation

In this section we express the collision kernel  $C(q_\perp)$  as a correlator supported on  $x^3 = x^0$  trajectories and evaluate it using EQCD. We only give details in the Feynman gauge  $\xi = 0$ , though we have explicitly verified the  $\xi$ -independence of our (gauge-invariant) collision kernel, as a check on the calculation.

### 4.1 Operator definition of $C(q_\perp)$ and leading order result

The evolution of the transverse momentum of a high-energy particle can be described by looking at its density matrix, as described in detail in [21]. For classical effects,

however (and even more so because we are taking the velocity to be  $v = 1 + \epsilon$ ), we can neglect operator ordering issues and replace the evolution of the density matrix by that of a dipole; we will come back to operator ordering issues in section 6.2.

High energy dipoles ( $E \gg m_D$ ) propagate eikinally in the soft classical background. The collision kernel describing the evolution of its transverse momentum can thus be recovered from the Fourier transform of the (long-time limit of the) dipole propagation amplitude  $W$  [28] [29] [39]:

$$\begin{aligned} W(t, x_\perp) &\sim e^{-tC(x_\perp) + \mathcal{O}(1)}, \quad t \rightarrow \infty, \\ \Leftrightarrow C(q_\perp) &\equiv \int d^2x_\perp e^{ip_\perp \cdot x_\perp} C(x_\perp). \end{aligned} \quad (9)$$

$C(q_\perp)$  is short for  $(2\pi)^2 d\Gamma/d^2q_\perp$ , as in (1). The dipole amplitude  $W(t, x_\perp)$  is given by the trace of a long, thin rectangular Wilson loop stretching along the light-cone coordinate  $x^+$ , with a small transverse extension  $x_\perp$  (see fig. 2).

The naive dimensional reduction of the Wilson loop (9) yields a Wilson loop stretching along the  $z$ -axis of the three-dimensional EQCD theory. It couples to the linear combination  $A_+ \equiv (A_z + A_0)$  of the EQCD fields, reflecting its ultrarelativistic origin. This “naive” dimensional reduction corresponds to keeping only the direct coupling to the  $n = 0$  modes. As explained in subsection 3.2, this will be justified provided we do not find ultraviolet divergences.

At the lowest order in perturbation theory, only the single-gluon exchange diagram ((a) of fig. 3) contributes,

$$\begin{aligned} C(q_\perp) &= g^2 T C_s \int_{-\infty}^{\infty} dz \int d^2x_\perp e^{ip_\perp \cdot x_\perp} \tilde{G}_{++}(z, x_\perp) \\ &= g^2 T C_s \tilde{G}_{++}(q_z = 0, q_\perp) = g^2 T C_s \left( \frac{1}{q_\perp^2} - \frac{1}{q_\perp^2 + m_D^2} \right), \end{aligned} \quad (10)$$

where we have used (8). The compact form (10) was first obtained by means of sum rules by Aurenche, Gelis and Zaraket [18], which we show in Appendix A are equivalent to our approach.

## 4.2 Diagram (b)

At the next-to-leading order (one-loop), self-energy insertions to the single-gluon diagram (b) contribute (we will often write “ $q_\perp$ ” for a three-vector with  $q_z = 0$ , which

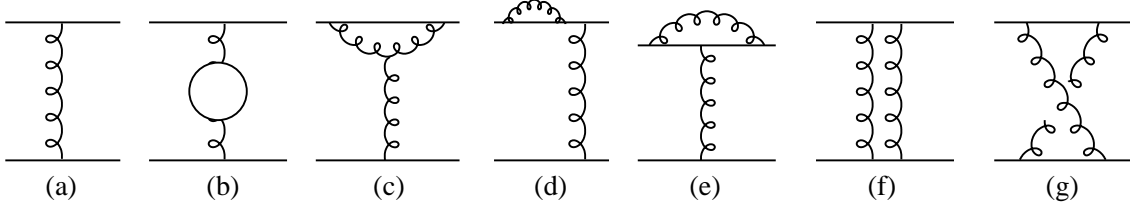


Figure 3: Tree and one-loop diagrams contributing to  $C(q_\perp)$ .

should cause no confusion; “ $\int_p$ ” is short for  $\int \frac{d^3 p}{(2\pi)^3}$ :

$$\begin{aligned}
C(q_\perp)_{(b)}/g^2 T C_s &= \frac{\delta\Pi^{00}(q_\perp)}{(q_\perp^2 + m_D^2)^2} - \frac{\delta\Pi^{zz}(q_\perp)}{q_\perp^4}, \\
\frac{\delta\Pi^{00}(q)}{g^2 T C_A} &= - \int_p \left[ \frac{(2q_\perp - p)^2}{p^2((q_\perp - p)^2 + m_D^2)} - \frac{3}{p^2} \right], \\
\frac{\delta\Pi^{zz}(q)}{g^2 T C_A} &= - \int_p \left[ \frac{2p_z^2}{(p^2 + m_D^2)((q_\perp - p)^2 + m_D^2)} - \frac{1}{p^2 + m_D^2} \right] \\
&\quad - \int_p \left[ \frac{3p_z^2 + 2q_\perp^2 + p^2}{p^2(q_\perp - p)^2} - \frac{2}{p^2} - \frac{p_z^2}{p^2(q_\perp - p)^2} \right]. \quad (11)
\end{aligned}$$

Each bracket includes the contributions of one fish and one tadpole diagram, while the last one also includes the ghost loop.

The (linear) ultraviolet divergences in (11) are to be canceled by matching counter-terms that can be unambiguously calculated within the framework of dimensional reduction [37, 38]. They merely represent the (hard thermal loop) coupling of the  $n \neq 0$  gluons to the soft  $n = 0$  ones, e.g. the gluon contribution to the  $A^0$  mass squared  $m_D^2$ . The fact that the direct coupling to exchange gluons with  $q^0 = q^3 \neq 0$  does not contribute to the divergences can also be checked explicitly, from the convergence, with respect to  $q^3$ , of the real-time integral (22) (this justifies making the soft approximation on  $q^0$ ). Thus the divergences in (11) do not signal the presence of “new contributions” beyond the EQCD effective theory, as discussed in section 3.2.

Employing dimensional regularization, the divergences simply go away<sup>8</sup> and the counter-terms are zero to  $\mathcal{O}(g)$  [38]. This way we obtain (all our arctangents run from 0 to  $\pi/2$ ):

$$\frac{C(q_\perp)_{(b)}}{g^4 T^2 C_s C_A} = \frac{-m_D - 2 \frac{q_\perp^2 - m_D^2}{q_\perp} \tan^{-1} \left( \frac{q_\perp}{m_D} \right)}{4\pi(q_\perp^2 + m_D^2)^2} + \frac{7}{32q_\perp^3} + \frac{m_D - \frac{q_\perp^2 + 4m_D^2}{2q_\perp} \tan^{-1} \left( \frac{q_\perp}{2m_D} \right)}{8\pi q_\perp^4} \quad (12)$$

<sup>8</sup> The dimensionally-regulated integrals (11) have poles in dimensions 2 and 4 but are finite and unambiguous in dimension 3.

### 4.3 Diagram (c)

Diagram (c) plus its permutation contribute:

$$\frac{C(q_\perp)_{(c)}}{g^4 T^2 C_s C_A} = \int_p \left[ \frac{2}{q_\perp^2 (p^2 + m_D^2) ((q_\perp - p)^2 + m_D^2)} - \frac{1}{(q_\perp^2 + m_D^2) p^2 ((q_\perp - p)^2 + m_D^2)} - \frac{1}{(q_\perp^2 + m_D^2) (p^2 + m_D^2) (q_\perp - p)^2} \right] \quad (13)$$

$$= \frac{-\tan^{-1}\left(\frac{q_\perp}{m_D}\right)}{2\pi q_\perp (q_\perp^2 + m_D^2)} + \frac{\tan^{-1}\left(\frac{q_\perp}{2m_D}\right)}{2\pi q_\perp^3} \quad (14)$$

In the Feynman gauge, there is no contribution involving only transverse gauge fields: such a contribution would involve the (trivial)  $zzz$  vertex. Eq. (13) is manifestly convergent.

### 4.4 Diagrams (d)-(g)

Our calculation is based on a quasiparticle expansion, e.g. we simply set on-shell the external legs of scattering diagrams. The relevant expansion parameter is  $g$ , e.g. the ratio of the scattering width  $\sim g^2 T$  to the scattering's natural frequency scale  $m_D$ . Thus in evaluating the external state corrections (d) we need only keep those effects which are not suppressed by the smallness of the width. A narrow resonance being described by just its position and the total area under it, this means that diagram (d), at  $\mathcal{O}(g)$ , produces only mass-shell corrections and wave-function renormalization factors. The (here imaginary) “mass-shell” corrections have no effects: they are identical for the initial and final states, so the “energy” (read  $z$ -momentum) transfer is zero in any case. The wave-function renormalization contribution is given by an energy derivative of the eikonal self-energy, and (e) is unambiguous, yielding respectively (including all diagrams of similar topology):

$$\begin{aligned} C(q_\perp)_{(d)} &= 2g^4 T^2 C_s^2 \tilde{G}_{++}(q_\perp) \int_p \tilde{G}_{++}(p) \frac{d}{dp_z} \frac{1}{p_z - i\epsilon} \\ C(q_\perp)_{(e)} &= 2g^4 T^2 C_s (C_s - \frac{1}{2} C_A) \tilde{G}_{++}(q_\perp) \int_p \tilde{G}_{++}(p) \frac{1}{(p_z - i\epsilon)^2} \end{aligned} \quad (15)$$

The sum of (d) and (e) is proportional to  $C_A$  and identically vanishes in the abelian theory ( $C_A = 0$ ), as required by abelian exponentiation<sup>9</sup>.

---

<sup>9</sup> Abelian Wilson loops, computed using Gaussian distribution for gauge fields (as is done by diagrams (d)-(g), for which only the two-point function of the gauge field enters), simply exponentiate:  $\langle e^{\int A} \rangle = \exp(\frac{1}{2} \langle \int A \int A \rangle)$ . As a consequence, the collision kernel as defined from (9) is tree-level exact in such theories; there is no interference between scattering events.

Part of diagram (f) is already included by the exponentiation of (10) (diagram (a)): this generates the approximation to (f) in which the intermediate eikonal propagators are put on-shell. To avoid double-counting, this must be subtracted. We must first regulate the associated “pinching” ( $q_z \rightarrow 0$ ) singularity, which we do by flowing a small external  $z$ -momentum  $\omega$  into the Wilson loop. We then take the limit  $\omega \rightarrow 0$  after the subtraction. Diagram (g) poses no difficulty.

$$C(q_\perp)_{(f)} = g^4 T^2 C_s^2 \int_p \tilde{G}_{++}(p) \tilde{G}_{++}(q-p) \left[ \frac{1}{(p_z + i\epsilon)(p_z + \omega - i\epsilon)} + \frac{2\pi i \delta(p_z)}{\omega - i\epsilon} \right]_{\omega \rightarrow 0} \quad (16)$$

$$C(q_\perp)_{(g)} = -g^4 T^2 C_s (C_s - \frac{1}{2} C_A) \int_q \frac{\tilde{G}_{++}(p) \tilde{G}_{++}(q_\perp - p)}{(p_z - i\epsilon)^2}. \quad (17)$$

Eq. (16) has a well-defined  $\omega \rightarrow 0$  limit, as follows from the identity  $1/(p_z + i\epsilon) - 1/(p_z - i\epsilon) = -2\pi i \delta(p_z)$ . This limit takes a form identical to (17) and the sum is proportional to  $C_A$ , again as required by abelian exponentiation. This confirms the correctness of our evaluation of (f).

The sum of diagrams (d)-(g) yields:

$$\frac{C(q_\perp)_{(d)\dots(g)}}{g^4 T^2 C_s C_A} = \frac{1}{2} \int_p \frac{\tilde{G}_{++}(p) \tilde{G}_{++}(q_\perp - p) - 2\tilde{G}_{++}(p) \tilde{G}_{++}(q_\perp)}{(p_z - i\epsilon)^2} \quad (18)$$

$$= \frac{m_D}{4\pi(q_\perp^2 + m_D^2)} \left[ \frac{3}{q_\perp^2 + 4m_D^2} - \frac{2}{(q_\perp^2 + m_D^2)} - \frac{1}{q_\perp^2} \right] \quad (19)$$

The function  $\tilde{G}_{++}$  is  $\tilde{G}_{00} + \tilde{G}_{zz}$ , as given in eq. (8). To evaluate (18) we have found convenient to first apply integration by parts to the  $1/(p_z - i\epsilon)^2$  denominator, which removes the explicit  $p_z$ -dependence and reduces the integral to a set of standard isotropic Feynman integrals. Eq. (18) is manifestly infrared- (and ultraviolet-) safe, upon enforcing  $p \leftrightarrow (q_\perp - p)$  symmetry.

## 4.5 Final formulae

In summary, we have obtained all  $\mathcal{O}(g)$  contributions to the collision kernel  $C(q_\perp)$ :

$$\begin{aligned} C(q_\perp)^{(\text{LO})} &= \frac{g^2 T C_s m_D^2}{q_\perp^2 (q_\perp^2 + m_D^2)} \\ \frac{C(q_\perp)^{(\text{NLO})}}{g^4 T^2 C_s C_A} &= \frac{7}{32q_\perp^3} + \frac{-m_D - 2\frac{q_\perp^2 - m_D^2}{q_\perp} \tan^{-1}\left(\frac{q_\perp}{m_D}\right)}{4\pi(q_\perp^2 + m_D^2)^2} + \frac{m_D - \frac{q_\perp^2 + 4m_D^2}{2q_\perp} \tan^{-1}\left(\frac{q_\perp}{2m_D}\right)}{8\pi q_\perp^4} \\ &\quad - \frac{\tan^{-1}\left(\frac{q_\perp}{m_D}\right)}{2\pi q_\perp (q_\perp^2 + m_D^2)} + \frac{\tan^{-1}\left(\frac{q_\perp}{2m_D}\right)}{2\pi q_\perp^3} \\ &\quad + \frac{m_D}{4\pi(q_\perp^2 + m_D^2)} \left[ \frac{3}{q_\perp^2 + 4m_D^2} - \frac{2}{(q_\perp^2 + m_D^2)} - \frac{1}{q_\perp^2} \right]. \end{aligned} \quad (20)$$

These expressions are valid for  $q_\perp \ll T$ . The leading order kernel for  $q_\perp \gtrsim T$  gets slightly modified, see (22).

The reader might wonder as to the appearance of arctangents with two distinct arguments in (20). They can be understood by looking in the complex  $q_\perp^2$ -plane:  $\tan^{-1}(q_\perp/2m_D)$  has a branch cut starting at  $q_\perp^2 = -4m_D^2$ , exhibiting its origin from the exchange of a pair of two quanta of mass  $m_D$  (longitudinal gluons). The branch cut of  $\tan^{-1}(q_\perp/m_D)$ , starting at  $q_\perp^2 = -m_D^2$ , arises from the exchange of one longitudinal and one transverse gluon. Both arctangents occur, since both of these pairs of states can be exchanged. Exchange of two massless quanta also occurs, and generates  $1/\sqrt{q_\perp^2}$ -type of discontinuities instead of arctangents.

## 5 Evaluation of $\hat{q}^{(\text{NLO})}$

The effective theory approach we have used so far is valid for  $q_\perp \ll T$ . As mentioned in section 2.3, however, the momentum broadening coefficient  $\hat{q}$  (second moment of  $C(q_\perp)$ ) receives contributions from all scales up to a process-dependent cut-off  $q_{\text{max}}$ . In this section we will assume<sup>10</sup>  $q_{\text{max}} \gg T$ .

To separate the soft and hard contributions to  $\hat{q}$ , we find convenient to introduce an auxiliary scale  $q^*$  obeying  $m_D \ll q^* \ll T$ :

$$\hat{q} = \int_0^{q^*} \frac{d^2 q_\perp}{(2\pi)^2} q_\perp^2 C(q_\perp)^{\text{soft}} + \int_{q^*}^{q_{\text{max}}} \frac{d^2 q_\perp}{(2\pi)^2} q_\perp^2 C(q_\perp)^{\text{hard}} \quad (21)$$

The soft kernel  $C(q_\perp)^{\text{soft}}$  is given by (20). The hard kernel  $C(q_\perp)^{\text{hard}}$  describes tree-level  $2 \rightarrow 2$  scattering processes against plasma constituents, with self-energy corrections omitted on the exchange gluon (since they represent only  $\sim g^2$  corrections for  $q_\perp \sim T$ ). The large particle energy  $E \gg T$  guarantees that the Mandelstam invariants  $s \sim ET$  and  $-t = q_\perp^2$  obey  $|t| \ll s$ , so that the relevant scattering matrix elements assume the universal (eikonal) form  $\propto s^2/t^2$ . The kinematics force  $q^0 = q_z$  for the momentum transfer  $q$ . In fact, these processes are precisely described by the central cut of the (four-dimensional) diagram (b) of fig. 3. Performing the  $q_z$  integration in the expression for the collision rate (as done in [17]; more details can be found in [26]), one obtains:

$$C(q_\perp)^{\text{hard}} = \frac{g^4 C_s}{q_\perp^4} \int \frac{d^3 p}{(2\pi)^3} \frac{p - p_z}{p} [2C_A n_B(p)(1 + n_B(p')) + 4N_f T_f n_F(p)(1 - n_F(p'))], \quad (22)$$

---

<sup>10</sup> In the context of jet quenching this is (parametrically) equivalent to  $E \gg T/g^4$ , with  $E$  the *smallest* energy of the participants.

with  $p, p'$  the initial and final momentum of the target particle;  $p' = p + q_z$ ,  $q_z = q^0 = \frac{q_\perp^2 + 2q_\perp \cdot p}{2(p - p_z)}$ . In the regime  $q_\perp \ll T$ ,  $p' \approx p$  and (22) reduces (as it must) to the large  $q_\perp$  limit of (10),  $C(q_\perp) \approx g^2 m_D^2 C_s T / q_\perp^4$ .

Integrating (22) over  $q$  to obtain the hard contribution to (21), and expanding it in powers of  $q^*/T$ , yields:

$$\begin{aligned} \frac{\hat{q}^{\text{hard}}}{g^4 C_s T^3} &= \frac{C_A}{6\pi} \left[ \log \left( \frac{T}{q^*} \right) + \frac{\zeta(3)}{\zeta(2)} \log \left( \frac{q_{\text{max}}}{T} \right) - 0.068854926766592 \dots + \frac{3}{16} \frac{q^*}{T} + \dots \right] \\ &+ \frac{N_f T_f}{6\pi} \left[ \log \left( \frac{T}{q^*} \right) + \frac{3}{2} \frac{\zeta(3)}{\zeta(2)} \log \left( \frac{q_{\text{max}}}{T} \right) - 0.072856349715786 \dots + \dots \right], \end{aligned} \quad (23)$$

with the omitted terms being suppressed by  $(q^*/T)^2$  or more. The quoted numbers are from [26]; we have verified the first five significant digits by direct numerical integration of (22)<sup>11</sup>. The  $\sim q^*/T$  term arises from soft bosons with  $p, p' \ll T$  and can be obtained in the soft approximation  $n_B(p), n_B(p') \rightarrow T/p, T/p'$ ; it is also given in [26].

The soft contribution to (21), e.g. the second moment of (20), admits the expansion:

$$\frac{\hat{q}^{\text{soft}}}{C_s} = \frac{m_D^2 g^2 T}{2\pi} \log \left( \frac{q^*}{m_D} \right) + \frac{g^4 T^2 C_A m_D}{2\pi} \left[ -\frac{q^*}{16m_D} + \frac{3\pi^2 + 10 - 4 \log 2}{16\pi} + \dots \right], \quad (24)$$

with the omitted terms being suppressed by powers of  $m_D/q^*$ . The  $q^*$  dependence of (23) and (24) cancels out in their sum, as it must do, producing the advertised formula (3). This cancellation provides a rather nontrivial check on the calculation.

The reader might inquire as to whether we have consistently included all  $\mathcal{O}(g)$  contributions to  $\hat{q}$ . Taking  $q^* \sim g^{1/2} T$ , for instance, the omitted terms  $\sim (q^*/T)^2$  in (23) might naively appear to be  $\mathcal{O}(g)$ , suggesting contributions from other, omitted terms.

Estimates of this kind can be misleading, however, because  $q^*$  is not a physical scale in this problem. The matching region  $m_D \ll q^* \ll T$  can be described equivalently using the low-energy description (EQCD) or the full theory, ensuring that  $q^*$  always disappears from final expressions. This is seen explicitly for the leading truncation errors  $\sim q^*/T$  in (23) and (24): instead of producing  $\mathcal{O}(g^{1/2})$  corrections, as one would naively expect setting  $q^* \sim g^{1/2} T$ , they cancel against each other and the leading correction is  $\mathcal{O}(g)$ , not  $\mathcal{O}(g^{1/2})$ . Since similar cancellations are bound to occur at all orders, this simply means that the scale  $q^*$  should not enter power-counting estimates. Because higher loop diagrams are  $\sim g^2$  when  $q_\perp \sim T$  and because we have included all  $\mathcal{O}(g)$  effects when  $q_\perp \sim m_D$ , we thus conclude that we have included all  $\mathcal{O}(g)$  contributions.

Finally, we note that, in the spirit of [40], we could have used dimensional regularization to separate the  $q$  integration, instead of the sharp cutoff  $q^*$ . In this scheme,

---

<sup>11</sup>I thank P. Arnold for pointing to me a numerical error in an early draft of this paper.



the hard  $q^*/T$  term in (23) disappears: there is no suitable dimensionful parameter to replace  $q^*$ . The  $\mathcal{O}(g)$  corrections then come solely from the (unambiguous) dimensionally-regulated soft integral (20).

## 6 Jet Evolution

We now extend the calculation to obtain the collision kernel relevant for bremsstrahlung and pair production processes. The new complication is that, except for QED processes, the relevant object to evolve in the plasma is no longer a “dipole”: it involves three charges. For instance, to describe the gluon bremsstrahlung process  $\psi \rightarrow g\psi$ , one must evolve an operator which annihilates a quark and creates a quark-gluon pair (see [28] [29] [30], which, however, use somewhat different notations):

$$\mathcal{O}_{\psi \rightarrow \psi g} = |\psi, g\rangle \langle \psi|. \quad (25)$$

The three color charges in (25) are paired together to form a color-singlet state, as dictated by the (DGLAP) gluon emission vertex which generates this operator.

It turns out that only one transverse momentum suffices to describe the internal state of (25). A priori the description of three charges might seem to require three momenta, but momentum conservation reduces this by one, and a symmetry removes yet another one: by suitably choosing the  $z$ -axis it is always possible to “gauge” to zero one of the transverse momenta (see the discussion preceding eq.(6.6) in [30]<sup>12</sup>). In the following, for concreteness, we shall gauge to zero the transverse momentum of particle 1, and  $q_\perp$  will refer to the transverse momentum of particle 2.

At the leading order, the relevant collision kernel is a sum over two-body contributions [28] [29] [30]:

$$\frac{d\Gamma_3(q_\perp)}{d^2q_\perp/(2\pi)^2} = \frac{C_2+C_3-C_1}{2} \tilde{C}(q_\perp) + \frac{C_1+C_3-C_2}{2} \tilde{C}\left(\frac{E_1}{E_2}q_\perp\right) + \frac{C_1+C_2-C_3}{2} \tilde{C}\left(\frac{E_1}{E_3}q_\perp\right) \quad (26)$$

with  $C_i$  and  $E_i$  respectively the Casimir and longitudinal momenta of the participating particles;  $\tilde{C}(q_\perp) \equiv \frac{1}{C_s}C(q_\perp)$  denotes a single-particle collision kernel with its Casimir factor stripped off; we recall that the LO (and NLO) kernels respect Casimir scaling. In the special limit in which one of the  $E_i$  becomes much smaller than the other ones, the motion of this particle dominates and the kernel (26) reduces to the one for single-particle diffusion,  $C(q_\perp)$ , for  $i = 2, 3$ , and  $C(\frac{E_1}{E_2}q_\perp)$  when  $i = 1$ .

As we presently show, it turns out that the formula (26) also holds at NLO, provided the NLO expression (20) for  $C(q_\perp)$  is used in it.

---

<sup>12</sup> For high-energy jets (when at least *one* of the energy of the participant is large,  $E_{\max} \gg T$ ), these rotations can be taken to have energy-suppressed angles  $\sim q_\perp/E$ , and thus to have negligible effects on the longitudinal momenta. Even when  $E_{\max} \sim T$ , the angles are at most  $\sim g$  and the changes in longitudinal momenta are  $\sim g^2$ , beyond the accuracy considered in this paper.

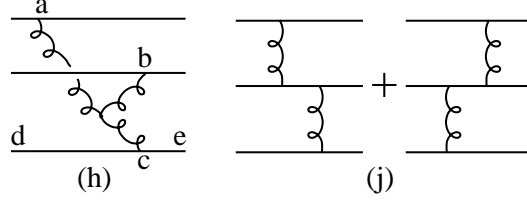


Figure 4: Additional diagrams for the evolution of a triplet of charges.

### 6.1 “Three-pole” propagation at NLO

To keep the discussion simple we will assume that particle 3 is a gluon (color adjoint state), which is sufficient to cover all splitting processes in QCD (and  $\mathcal{N} = 4$  super Yang-Mills). This ensures that particles 1 and 2 are antiparticles to each other. We denote by  $|s\rangle$  the relevant singlet state in the tensor product of the three charges; explicitly,  $|s\rangle$  is given by the representation matrices  $(t_1)_{ij}^a$ .

The previously treated dipole diagrams (a)-(g) must now be summed over the three possible pairs of particles, and we must recompute their group theory factors. Diagrams (a)-(b) involve, in the case the interaction is between particles 1 and 2 [30],

$$-\langle s | t_1^a \otimes t_2^a | s \rangle = \langle s | \frac{t_1^a t_1^a + t_2^a t_2^a - (t_1 + t_2)^a (t_1 + t_2)^a}{2} | s \rangle = \frac{C_1 + C_2 - C_3}{2}, \quad (27)$$

which reproduces the structure (26), upon summing over pairs and using rotational invariance to “gauge” to zero particle 1’s  $\perp$ -momentum. Diagrams (c)-(g) fit the same structure, as follows from the fact that they organize themselves into commutators. For instance,

$$\begin{aligned} (c) &\propto i f^{abc} \langle s | t_1^a t_1^b \otimes t_2^c | s \rangle = -\frac{C_A}{2} \langle s | t_1^a \otimes t_2^a | s \rangle, \\ (f) + (g) &\propto \langle s | [t_1^a, t_1^b] \otimes \frac{[t_2^a, t_2^b]}{2} | s \rangle = -\frac{C_A}{2} \langle s | t_1^a \otimes t_2^a | s \rangle. \end{aligned} \quad (28)$$

Here we have used the identities  $[t^a, t^b] = i f^{abc} t^c$  and  $f^{abc} f^{abc'} = C_A \delta^{cc'}$ .

There are also new diagrams (fig. 4), which couple together the three particles nontrivially. In diagram (h) (see fig. 4), the Yang-Mills 3-vertex generates a factor  $f^{abc}$  and the coupling to the gluon line is given by  $(t_3)_{de}^c \propto f^{cde}$ , whence:

$$(h) = \langle s | t_1^a t_2^b t_3^c | s \rangle f^{abc} \propto \text{Tr}_1 (t^a t^d t^b t^e) f^{abc} f^{dec} = 0, \quad (29)$$

with the trace taken in the representation of the particle 1. We could prove this identity by making extensive use of the antisymmetry of the  $f^{abc}$ . Diagrams (i) are similar to

diagram (g) treated in subsection 4.4, and the main point is that there is a sign between the two diagrams, due to the reversed middle propagator, thus yielding zero:

$$(i) \propto \langle s | t_1^a \otimes [t_2^a, t_2^b] \otimes t_3^b | s \rangle = 0. \quad (30)$$

Thus the new diagrams (h)-(i) vanish and the factorization formula (26) remains valid at NLO.

We view this as somewhat surprising; this could be an artefact of the relatively low order in perturbation theory to which we are working.

## 6.2 Discussion of operator ordering issues

We now briefly discuss operator ordering issues, for the Wilson lines in (9) and their three-particle generalization (25). Although this is not directly relevant to the purely classical effects which are the main object of this paper, since nonperturbative definitions of  $\hat{q}$  have been used in the literature [21] [19] we feel that a discussion of them can be of interest.

To help clarify the physical significance of these issues, let us first consider, in QED, the processes of photon bremsstrahlung from a charge and of pair production from a photon. These processes differ in that the former takes place within the electromagnetic field generated by the initial charge, but the latter takes place in an essentially undisturbed medium (the induced field being suppressed by the small size of the produced dipole). The collision kernels relevant to these two processes could thus be different, due to the different backgrounds, and should be defined differently. In the eikonal regime, it is the role of the Wilson lines trailing behind the charges to source the backgrounds, which requires that they be properly ordered.

The proper ordering can be readily described using the language of the Schwinger-Keldysh “doubled fields” [41], in which amplitudes and their complex conjugate are described by type-1 and type-2 fields, respectively. For photon bremsstrahlung, evolving the relevant  $|\psi\gamma\rangle\langle\psi|$  matrix element requires one type-1  $\psi$  (and  $\gamma$ ) and one type-2  $\bar{\psi}$  field, whereas for pair production, evolving  $|\psi\bar{\psi}\rangle\langle\gamma|$  requires both charged fields to be type-1 (and  $\gamma$  to be type-2). In the latter case the Wilson lines nearly cancel against each other (for a small dipole), whereas in the former case they fail to cancel, due to operator ordering issues (they live on different branches of the Keldysh contour): instead they source an electromagnetic field. This reproduces the expected physics.

The story for QCD must be similar: for instance, evolving a  $|\psi, g\rangle\langle\psi|$  operator, relevant for gluon bremsstrahlung, should require type-1  $\psi$  and  $g$  fields, and a type-2  $\bar{\psi}$  field, with the obvious replacements to be made for other processes. Thus we see that the strong coupling calculations of the momentum broadening coefficient in [21] and [22], strictly speaking, gives a  $\hat{q}$  applicable to *photon* bremsstrahlung, whereas

the “jet quenching parameter” defined in [19], being defined from a space-like limit of correlators, is by hypothesis independent of operator ordering.

It is not clear, at least to the author, the extend to which these effects can be numerically important. Obviously, at weak coupling, they are suppressed by a power of the coupling (the preceding subsection shows that the suppression is at least  $\sim g^2$ ). Furthermore, in the  $v \nearrow 1$  limit relevant to high-energy jets, an argument based on the shrinking down of the “causal diamond” enclosing any two points on the trajectory of the jet might suggest that these effects disappear — e.g. there is no time available for the induced field to influence the jet back again; a rigorous analysis, in particular of quantum effects, will not be attempted here.

## 7 Acknowledgements

I am indebted to Guy D. Moore for useful discussions, and to P. Arnold for sharing an early draft of his work [26]. This work was supported in part by the Natural Sciences and Engineering Research Council of Canada.

## A Relation to sum rule approach

In this Appendix, we consider the problem of calculating, directly in four dimensions, the leading order collision kernel (9):

$$C(q_\perp)/g^2 C_s = \int \frac{dq_z}{2\pi} G_{++}^>(q^0 = q_z, q_\perp) \quad (31)$$

with  $q_\perp \ll T$ , and  $G_{++}$  the full HTL-resummed propagator [14]. The simple result (10) for it has been obtained previously using a sum rule by Aurenche, Gelis and Zaraket (AGZ) [18], and our aim here is to establish the equivalence between our approaches.

### A.1 Causality and Sum Rules

Due to causality, retarded correlators  $G^R(Q)$  must be analytic functions of the four-momentum  $Q$  when positive time-like or light-like imaginary four-vectors are added to it. This statement extends, in a Lorentz-covariant way, the familiar analyticity of  $G^R$  in the  $q^0$  upper-half plane [36].

Light-like imaginary parts are also allowed, because causality is preserved along light-fronts (e.g.  $G^R(x^+)$  vanishes for negative light-cone time  $x^+$ ).

In the classical approximation  $n_B(q^0) \approx T/q^0$ , (31) becomes:

$$(31) = T \int \frac{dq_z}{2\pi} \frac{G_{++}^R(q^0 = q_z, q_\perp) - G_{++}^A(q^0 = q_z, q_\perp)}{q_z}. \quad (32)$$

To evaluate this by contour integration, we first move the  $q_z = 0$  pole slightly off-axis,  $1/q_z \rightarrow 1/(q_z - i\epsilon)$ , which does not change the result since  $(G^R - G^A)$  vanishes at  $q_z = 0$ . Next, we note, using the standard HTL expressions [14], that  $G_{++}^{R,A}$  vanishes (like  $1/q_z^2$ ) at large  $|q_z|$ , making it possible to close integration contours at infinity. Closing the contour for  $G^R$  (resp.  $G^A$ ) in the upper (resp. lower) half-plane, one obtains a unique residue  $iTG_{++}^R(q^0 = q_z = 0, q_\perp)$  from  $G^R$  and nothing from  $G^A$ , due to their aforementioned analyticity properties, thus reproducing (10):

$$(31) = T \left( \frac{1}{q_\perp^2} - \frac{1}{q_\perp^2 + m_D^2} \right). \quad (33)$$

Additional poles at the Matsubara frequencies  $q^0 = q_z = 2\pi inT$  would have appeared in this result, in agreement with the sum (7), had we kept the full Bose distribution function  $n_B(q^0)$ . This shows that the classical approximation to distribution functions is equivalent to keeping only the  $n = 0$  Matsubara frequency.

More generally, at higher orders in perturbation theory one could also imagine computing the dipole amplitude (9) using the real-time formalism. The fact that the operator of interest is supported at a constant value of  $x_+$  allows the integral over the conjugate momentum  $q^+$  to be performed by contour integration, in the same way that integrals over  $q^0$  (or equivalently, the sum-integrals of the imaginary-time formalism) would be done for equal-time correlators [36]. In addition to standard gauge field propagators, the integrands to be met also involve eikonal propagators  $\sim 1/q^-$ ; but since they do not depend on  $q^+$  they would not interfere with this calculation. Thus, as claimed in the text, we can also derive all the results of section 4 using causality-based sum rules. This is in fact how we first obtained them. It is also clear that, in general, making the approximation  $n_B(p^0) \rightarrow p^0/T$  in all propagators in real-time is equivalent to dropping all  $n \neq 0$  Matsubara modes.

## A.2 AGZ's sum rule

AGZ [18] study exactly the integral (31), but parametrized using a different variable,  $x = q^0/q$  (so  $q^0(x) = q_z(x) = |q_\perp|x/\sqrt{1-x^2}$ ):

$$(31) = |q_\perp| \int_{-1}^1 \frac{dx}{2\pi(1-x^2)^{3/2}} G_{++}^>(x, q_\perp) \quad (34)$$

A key observation in [18] is that the HTL propagators, viewed as a function of  $x$  with  $q_\perp$  fixed and  $q^0 = q_z$ , are analytic in the whole complex  $x$ -plane, apart from a branch cut at real  $x \in [-1, 1]$ . Using methods of complex analysis, they could then derive the result (33).

To show that this analyticity property in  $x$  is equivalent to the analyticity in  $q^+$  that we have used above (e.g. to causality), we rewrite the change of variable above

(34) as:

$$q^0(x) = q_z(x) = i|q_\perp| \frac{x}{\sqrt{x^2 - 1}}, \quad (35)$$

and choose to put the branch cut of the square root at real  $x \in [-1, 1]$ . Thus  $q^0 \rightarrow i|q_\perp|$  as  $|x| \rightarrow \infty$  in any direction. This choice of branch cut ensures that  $G^R(q^0(x), q_z(x), q_\perp)$  goes into the standard retarded function as  $\text{Im } x \rightarrow 0^+$ , and is consistent with the conventions of [18], e.g. this function has the same analytic structure as the  $G^R(x, q_\perp)$  of [18]. Careful inspection of (35) then reveals that the imaginary part of  $q^0$  is *positive* for all  $x$ , establishing that analyticity in  $x$  (for  $q^0 = q_z$  and at fixed  $q_\perp$ ) is a consequence of the above-discussed analyticity in  $q^+$ . It thus applies to any propagator, extending the claim of [18].

The authors of [18] worked in the Coulomb gauge and found, at intermediate steps, contributions from the large circle at  $|x| = \infty$  (proportional to  $1/(q_\perp^2 + \frac{1}{3}m_D^2)$ ), which in the end, precisely canceled out between the longitudinal and transverse channels. Since no such term has appeared in our approach, the reader might wonder as to their claimed equivalence. What happens is that these contributions are mere gauge artefacts; this also explains their ultimate cancellation. To see this, we note that the residue at  $|x| \rightarrow \infty$  corresponds to a pole at  $q^0 = q_z = iq_\perp$ , which is at an ordinary point in the upper-half  $q^+$ -plane and is thus forbidden by causality. But since a gauge like the Coulomb gauge does not respect causality in a Lorentz-covariant sense (its  $A^0$  field mediates an instantaneous Coulomb interaction), such poles are not forbidden in individual, gauge-dependent terms. They are bound, however, to cancel out in physical quantities like  $C(q_\perp)$ . Our approach assumes Lorentz-covariant causality from the start and cannot detect such unphysical contributions.

These complications, associated with causality violations in non-covariant gauges (in intermediate expressions), are easily avoided by working in a covariant gauge.

## References

- [1] K. Adcox *et al.* [PHENIX Collaboration] Phys. Rev. Lett. **88** 022301 (2003).
- [2] C. Adler *et al.* [STAR Collaboration] Phys. Rev. Lett. **89** 202301 (2002).
- [3] S. A. Bass, C. Gale, A. Majumder, C. Nonaka, G. Y. Qin, T. Renk and J. Ruppert, arXiv:0808.0908 [nucl-th].
- [4] P. Arnold and C. x. Zhai, Phys. Rev. D **51**, 1906 (1995) [arXiv:hep-ph/9410360].
- [5] E. Braaten and A. Nieto, Phys. Rev. Lett. **76**, 1417 (1996) [arXiv:hep-ph/9508406].

- [6] K. Kajantie, M. Laine, K. Rummukainen and Y. Schroder, Phys. Rev. D **67**, 105008 (2003) [arXiv:hep-ph/0211321]; F. Di Renzo, M. Laine, V. Miccio, Y. Schroder and C. Torrero, JHEP **0607**, 026 (2006) [arXiv:hep-ph/0605042].
- [7] H. Schulz, Nucl. Phys. B **413** 353 (1993)
- [8] M. E. Carrington, A. Gynther and D. Pickering, Phys. Rev. D **78**, 045018 (2008) [arXiv:0805.0170 [hep-ph]].
- [9] J. P. Blaizot, E. Iancu and A. Rebhan, Phys. Rev. D **63**, 065003 (2001) [arXiv:hep-ph/0005003].
- [10] S. Caron-Huot and G. D. Moore, Phys. Rev. Lett. **100**, 052301 (2008) [arXiv:0708.4232 [hep-ph]]; S. Caron-Huot and G. D. Moore, JHEP **0802**, 081 (2008) [arXiv:0801.2173 [hep-ph]].
- [11] M. Laine and Y. Schroder, JHEP **0503**, 067 (2005) [arXiv:hep-ph/0503061].
- [12] J. P. Blaizot, E. Iancu and A. Rebhan, Phys. Rev. D **68**, 025011 (2003) [arXiv:hep-ph/0303045].
- [13] K. Kajantie, M. Laine, K. Rummukainen and Y. Schroder, Phys. Rev. Lett. **86**, 10 (2001) [arXiv:hep-ph/0007109].
- [14] E. Braaten and R. D. Pisarski, Nucl. Phys. B **337**, 569 (1990); J. Frenkel and J. C. Taylor, Nucl. Phys. B **334**, 199 (1990).
- [15] J. P. Blaizot and E. Iancu, Phys. Rept. **359**, 355 (2002) [arXiv:hep-ph/0101103].
- [16] P. F. Kelly, Q. Liu, C. Lucchesi and C. Manuel, Phys. Rev. D **50**, 4209 (1994)
- [17] E. Braaten and M. H. Thoma, Phys. Rev. D **44**, 2625 (1991); Phys. Rev. D **44**, 1298 (1991).
- [18] P. Aurenche, F. Gelis and H. Zaraket, JHEP **0205**, 043 (2002) [arXiv:hep-ph/0204146].
- [19] H. Liu, K. Rajagopal and U. A. Wiedemann, Phys. Rev. Lett. **97**, 182301 (2006) [arXiv:hep-ph/0605178].
- [20] H. Liu, K. Rajagopal and Y. Shi, JHEP **0808**, 048 (2008) [arXiv:0803.3214 [hep-ph]].
- [21] J. Casalderrey-Solana and D. Teaney, JHEP **0704**, 039 (2007) [arXiv:hep-th/0701123].

- [22] S. S. Gubser, Nucl. Phys. B **790**, 175 (2008) [arXiv:hep-th/0612143].
- [23] Y. Hatta, E. Iancu and A. H. Mueller, JHEP **0805**, 037 (2008) [arXiv:0803.2481 [hep-th]].
- [24] S. S. Gubser, D. R. Gulotta, S. S. Pufu and F. D. Rocha, arXiv:0803.1470 [hep-th].
- [25] P. M. Chesler, K. Jensen, A. Karch and L. G. Yaffe, arXiv:0810.1985 [hep-th].
- [26] P. Arnold and W. Xiao, arXiv:0810.1026 [hep-ph].
- [27] G. Y. Qin, J. Ruppert, C. Gale, S. Jeon, G. D. Moore and M. G. Mustafa, Phys. Rev. Lett. **100**, 072301 (2008) [arXiv:0710.0605 [hep-ph]].
- [28] R. Baier, Y. L. Dokshitzer, S. Peigne and D. Schiff, Phys. Lett. B **345**, 277 (1995) [arXiv:hep-ph/9411409]. R. Baier, Y. L. Dokshitzer, A. H. Mueller, S. Peigne and D. Schiff, Nucl. Phys. B **483**, 291 (1997) [arXiv:hep-ph/9607355].
- [29] B. G. Zakharov, JETP Lett. **65**, 615 (1997) [hep-ph/9704255]; **63** 952 (1996) [hep-ph/9607440].
- [30] P. Arnold, G. D. Moore and L. G. Yaffe, JHEP **0206**, 030 (2002) [arXiv:hep-ph/0204343].
- [31] L. D. Landau and I. Pomeranchuk, Dokl. Akad. Nauk Ser. Fiz. **92** (1953) 535; L. D. Landau and I. Pomeranchuk, Dokl. Akad. Nauk Ser. Fiz. **92** (1953) 735; A. B. Migdal, Dokl. Akad. Nauk S.S.S.R. **105**, 77 (1955); A. B. Migdal, Phys. Rev. **103**, 1811 (1956).
- [32] S. Jeon and G. D. Moore, Phys. Rev. C **71**, 034901 (2005) [arXiv:hep-ph/0309332].
- [33] V. N. Gribov and L. N. Lipatov, Sov. J. Nucl. Phys. **15** (1972) 438; V. N. Gribov and L. N. Lipatov, Sov. J. Nucl. Phys. **15** (1972) 675; L. N. Lipatov, Sov. J. Nucl. Phys. **20** (1975) 94; G. Altarelli and G. Parisi, Nucl. Phys. **B126** (1977) 298; Yu. L. Dokshitzer, Sov. Phys. JETP **46** (1977) 641.
- [34] P. Arnold and C. Dogan, arXiv:0804.3359 [hep-ph].
- [35] A. Majumder, arXiv:0810.1367 [nucl-th].
- [36] J. I. Kapusta and C. Gale, *Cambridge, UK: Univ. Pr. (2006) 428 p.*
- [37] T. Appelquist and R. D. Pisarski, Phys. Rev. D **23**, 2305 (1981).
- [38] K. Farakos, K. Kajantie, K. Rummukainen and M. E. Shaposhnikov, Nucl. Phys. B **425**, 67 (1994) [hep-ph/9404201].



- [39] Z. t. Liang, X. N. Wang and J. Zhou, Phys. Rev. D **77**, 125010 (2008) [arXiv:0801.0434 [hep-ph]].
- [40] L. S. Brown, Phys. Rev. D **62**, 045026 (2000) [arXiv:physics/9911056].
- [41] J. Schwinger, J. Math. Phys. 2, 407 (1961), L. V. Keldysh, Sov. Phys. JETP 20, 1018 (1964).